DOI: http://dx.doi.org/10.22104/ijhfc.2015.176

*Iranian Journal of Hydrogen & Fuel Cell 4(2014) 247-260*

Iranian Journal of Hydrogen & Fuel Cell

IJHFC

Journal homepage://ijhfc.irost.ir

# Modeling of multi-population microbial fuel and electrolysis cells based on the bioanode potential conditions

**Masih Karimi Alavijeh[1], Mohammad Mahdi Mardanpour[1], Soheila Yaghmaei[1,*]**

[1]Department of Chemical and Petroleum Engineering, Sharif University of Technology, Azadi Avenue, P.O. Box 11365-9465, Tehran, Iran

**Article Information**

Article History:

Received:
21 June 2015
Received in revised form:
29 August 2015
Accepted:
12 September 2015

**Keywords**

Microbial fuel cell
Microbial electrolysis cell
Simulation
Anode potential.

**Abstract**

Microbial fuel cell and microbial electrolysis cell are two major types of microbial electrochemical cells. In the present study, we governed modeling of these systems by concentrating on the simulation of bioelectrochemical reactions in both biofilm and anolyte and considering the effect of pH on the microbial growth. The simulation of microbial fuel and electrolysis cells can be described by shifting the bioanode surface potential boundary conditions. Model validation was performed using experimental results from the MFC fed with cheese whey wastewater and then it was switched to a supposed microbial electrolysis cell. The effect of applied voltage as well as poising the cathode surface potential on the anode surface potential and microbial population have been acquired. The results showed that hydrogen production rate increases at the higher applied voltage and cathode potential, but the influence of cathode potential at the applied voltage of 0.9 V was much more tangible. The MFC was simulated in different pH values to optimize the power generation. The maximum of power output at 100 Ω was obtained in pH 7.5. In addition, the microbial behavior in the biofilm and anolyte was investigated as a strong function of pH. Due to the higher growth rate of electrogens, the optimum pH for the mixed culture of electrogens was the same for the pure culture (pH 7.7), but it was altered for acetoclstic methanoges.

## 1. Introduction

The microbial electrochemical cell (MXC) is regarded as an energy harvesting effort coupled with renewable energy stored in organic substances, and in the case of wastewater a generator of power or hydrogen while simultaneously treating wastewater. Bio-electrochemical oxidation of organic matters is a relatively new approach to directly obtain innate bioenergy accumulated in the matter through devices called microbial fuel cells (MFCs) and microbial electrolysis cells (MECs) by virtue of being able to acquire higher hydrogen production yields [1]. In MFCs, organic substances are degraded by bacteria as a biocatalyst and an electron is produced by anode respiring bacteria or electrogens [2]. This bacterial

*Corresponding Author's Tel.: +982166166430; fax:+982166166430
E-mail address: yaghmaei@sharif.edu (S. Yaghmaei)

group can transfer electrons to the surface of the anode by redox mediators or microbial interconnected nanowires [3]. Actually, MECs are recognized as modified MFCs that produce hydrogen as an energy carrier in a thermodynamically favorable way [4]. While a substantial number of modifications like integrated methods [5], three-dimensional graphite anodes [6], commercial cathode materials [7] and optimization of operating conditions such as external applied voltage [8] have been performed to enhance hydrogen production in MECs, knowledge about the MXC performance and biocatalyst behavior is not yet sufficient. Mathematical modeling can open a commercially new and fast solution to obviate some experimental limitations and predict the system performance by focusing on the simulation of indigenous reactions and mass transports in both MFCs and MECs. MFCs modeling is one of the most unresolved research subjects in recent years. Some of this research is concerned with more comprehensive views and have relative heavier mathematical calculations to investigate the different phenomena in MFCs. In the research by Picioreanu et al. [9-11], ageneral model to describe bioelectrochemical interactions in an MFC based on the electron transfer by a redox mediator with biofilm and anolyte simulation is developed. But due to many missing constants, its applicability is limited to only simple substrates, not complex ones. Pinto et al. [12] introduced a far simpler mediator-based model based only on the time-dependent equations while disregarding the spatial distributions. In this model the effect of methanogens presence on the electroactive microorganisms is inspected. The importance of the substrate and microorganisms spatial distributions in the biofilm as a conductive porous media is analyzed in a research by Kato Marcus et al. [13], and is applicable for a poised anode MFC. Sedaqatvand et al. [14], keeping the simplicity and the same approach, extended this model to a general anode potential status and complex wastewater. In these studies, competition between methanogens and electrogens as well as suspended cells modeling are not included in either model.

Although there have been several MFCs modeling studies, extensive MEC simulation of has not been performed. The multi-population model of MEC by Pinto et al. [15] is recognized as the sole MEC simulation model [15]. It is governed based on the same approaches in the previously published work [12].

In the present work, we introduced a combination of viewpoints to construct a general model which is able to simulate the dynamical performance of complex fuel-fed MXCs (including both MFCs and MECs) in a conductive biofilm. This model was able to estimate the different variables in the biofilm and the liquid bulk such as the spatial distribution of substrates and intermediates as well as miscellaneous microorganisms in the biofilm, concentration of substrates and microorganisms in the anolyte, biofilm thickness, potential distribution, etc.

## 2. Model equations

The model equations were established based upon the kinetics rates and biochemical and electrochemical mass balances in both anolyte and biofilm. Figure 1 shows the method used to govern model equations. According to this figure, owing to the typically large sized hydrolysable materials in wastewater, digestion of wastewater occurs dominantly in the anolyte (described by Equation (1), (20) and (21) in section 2.1 and 2.3) and due to the assumption that electrons are transferred by the conduction-based mechanism, not a mediated transfer, electrogens are considered to exist only in the biofilm (presented in Equation (3) and (12) in section 2.1 and 2.2). In contrast, acetoclastic methanogens can be present in both biofilm and anolyte (presented in Equation (2), (4), (13) and (23)). Wastewater is digested to acetate (through Equation (22)), as the dominant carboxylic acid end product in the anaerobic digestion process [16, 17], and then the acetate diffuses through the porous biofilm (described by Equation (9)). Electrons depart across the biofilm to the anode surface under the electrical potential difference (presented by Equation (19)), which is

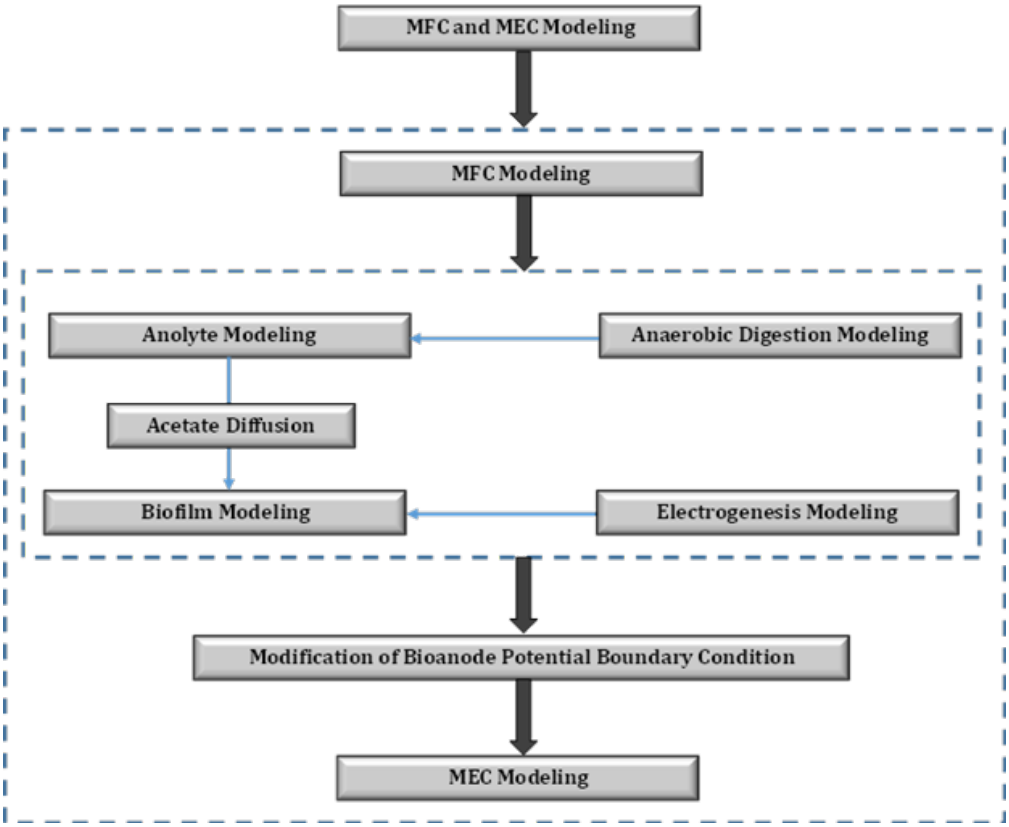


**Fig. 1. The method used to govern model equations which are established based upon the kinetics rates and biochemical and electrochemical mass balances in both anolyte and biofilm.**

described by Ohm's law, which is similar to Fick's law. The anode surface potential is influenced by the external electrical load (for MFC) or applied voltage (for MEC). By modification of the anode potential boundary condition, the model can be changed to simulate an MEC (through Equation (27)).

### 2. 1. Rate equations

Rates of substrate consumption in the anolyte including wastewater degradation and acetate consumption as well as acetate consumption in the biofilm are described by the Monod equation. As electrogens respire by transferring produced electrons to a final oxidant or electrons acceptor (i.e. anode surface), dual-limitation Monod kinetics is used to express the rate of acetate consumption by electrogens in the biofilm (Equation (3)). An empirical function denoted by "$I_{pH}$" is used to consider the effect of pH on the growth of three microbial groups (fermentative bacteria, acetoclastic methanogens and electrogens) [18]. According to this function the growth should be optimum between the lower and upper limits of pH ($pH_{LL}$ and $pH_{UL}$) and inhibited beyond this interval. Some electrogens can utilize dead microbes when there is a lack of organic matter and produce a bit of electron flow. This phenomenon is recognized as endogenous respiration (presented by Equation (8)). Microbial inactivation rates are described by first-order kinetics (through Equation (5) to (7)).
Wastewater and bulk acetate consumption rates are written as follows [12]:

$$q_{ww} = q_{ww,\max} C_F \left( \frac{S_{WW}}{S_{WW} + K_{WW}} \right) I_{pH,F}$$
$$I_{pH,F} = \left( \frac{1 + 2 \times 10^{0.5(pH_{LL,F} - pH_{UL,F})}}{1 + 10^{(pH - pH_{UL,F})} + 10^{(pH_{LL,F} - pH)}} \right) \quad (1)$$

$$q_{Ac,AM,bulk} = q_{Ac,AM,\max} \left( \frac{S_{Ac,bulk}}{S_{Ac,bulk} + K_{Ac,AM}} \right) I_{pH,AM}$$
$$I_{pH,AM} = \left( \frac{1 + 2 \times 10^{0.5(pH_{LL,AM} - pH_{UL,AM})}}{1 + 10^{(pH - pH_{UL,AM})} + 10^{(pH_{LL,AM} - pH)}} \right) \quad (2)$$

Acetate consumption rate in the biofilm is expressed by Equation (3) and (4) [13]:
rate to be cooled. This can be explained by the more efficient the system is the less heat it will lose, and therefore, needless cooling water mass flow rate.

$$q_{AC} = q_{AC,E,\max} \phi_{E,a} \left( \frac{S_{AC}}{S_{AC} + K_{AC,E}} \right) \left( \frac{1}{1 + \exp\left( \frac{-F}{RT} \eta \right)} \right) I_{pH,E}$$
$$I_{pH,E} = \left( \frac{1 + 2 \times 10^{0.5(pH_{LL,E} - pH_{UL,E})}}{1 + 10^{(pH - pH_{UL,AM})E} + 10^{(pH_{LL,E} - pH)}} \right) \quad (3)$$

$$q_{AC,AM} = q_{AC,AM,\max} \phi_{AM,a} \left( \frac{S_{AC}}{S_{AC} + K_{AC,AM}} \right) \quad (4)$$

Inactivation rates are as follows [12, 13]:

$$r_{ina,j} = b_{ina,j} \phi_{i,a} \quad (5)$$

$$r_{ina,bulk,AM} = b_{ina,AM} C_{AM} \quad (6)$$

$$r_{ina,F} = b_{ina,F} C_F \quad (7)$$

Endogenous respiration rate is expressed as follows [13]:

$$r_{res} = b_{res} \phi_{E,a} \left( \frac{1}{1 + \exp\left( \frac{-F}{RT} \eta \right)} \right) \quad (8)$$

### 2. 2. Biofilm mass balances

Diffusion of acetate into the biofilm is recognized as the dominant transport mechanism in this media. In addition, with respect to the far smaller characteristic time of acetate consumption in comparison with microbial growth, the acetate mass balance equation can be estimated as a pseudo-steady-state equation (Equation (9)) [19]. In this equation, the first term illustrates diffusive transport and the two other terms are acetate consumption rates by the electrogens and acetoclastic methanogens, respectively:

$$D_{Ac,f} \frac{\partial^2 S_{Ac}}{\partial z^2} - X_{E,a} q_{Ac,E} - X_{AM,a} q_{Ac,AM} = 0 \quad (9)$$

Boundary conditions of Equation (9) are expressed as follows:

• No flux at the anode surface:

$$\frac{\partial S_{Ac}}{\partial z} |_{z=0} = 0 \quad (10)$$

• Interphase mass transfer at the biofilm/anolyte interface:

$$D_{Ac,f} \frac{dS_{Ac}}{dz} |_{z=L_f} = \left( \frac{D_{Ac,l}}{L} \right) \left( S_{Ac,bulk} - S_{Ac,surface} \right) \quad (11)$$

Active microorganisms advective mass balances in the biofilm can be written as Equation (12) for the electrogenic bacteria and Equation (13) for the acetoclastic methanogenic bacteria (19):

$$\frac{\partial \phi_{E,a}}{\partial t} + \frac{\partial \left( v \phi_{E,a} \right)}{\partial z} = Y_E q_{Ac,E} - r_{res} - r_{ina,E} = \mu_{E,a} \quad (12)$$

$$\frac{\partial \phi_{AM,a}}{\partial t} + \frac{\partial \left( v \phi_{AM,a} \right)}{\partial z} = Y_{AM} q_{Ac,AM} - r_{ina,AM} = \mu_{AM,a} \quad (13)$$

Equation (12) and (13) are solved subject to Equation (14) as the surface of the anode is a stationary anode:

$$v|_{z=0} = 0 \tag{14}$$

By the same method as that for active microorganisms, the mass balance equation for inactive microorganisms j in the biofilm is as follows:

$$\frac{\partial \phi_{j,i}}{\partial t} + \frac{\partial \left(v \phi_{j,i}\right)}{\partial z} = \frac{X_{j,a}}{X_{j,i}} r_{ina,j} = \mu_{j,i} \tag{15}$$

Local biofilm advective velocity differential equation (which can be derived by the sum of Equation (12), (13) and (15) as the total mass balance) are presented as follows:

$$\frac{\partial v}{\partial z} = \sum_{j} \left(\mu_{j,a} + \mu_{j,i}\right) \tag{16}$$

The time-variable differential equation of biofilm thickness variation is expressed as Equation (17). As can been seen from Equation (17), the biofilm thickness can be increased by advective velocity and decreased by the detachment phenomenon [13]:

$$\frac{dL_f}{dt} = v\left(t, L_f\right) - b_{det} L_f \tag{17}$$

Ohm's law is used to describe the current density in response to the electric field and is written by Equation (18) [20]:

$$j = -\kappa_{bio} \frac{d\eta}{dz} \tag{18}$$

Potential spatial distribution differential equation in the biofilm or the electron mass balance is defined as follows [13]:

$$\kappa_{bio} \frac{d^2\eta}{dz^2} - \frac{F \gamma_1}{\tau} f_e^0 X_{E,a} q_{Ac,E} - \frac{F \gamma_2}{\tau} X_{E,a} r_{res} = 0 \tag{19}$$

It should be noted that the second and third terms denote electron generation by acetate consumption and endogenous respiration, respectively.

### 2. 3. Anolyte mass balances

By assuming a well-mixed and batch mode for an anode compartment anolyte, the mass balances of the substrates are defined as follows:

$$\frac{\partial S_{WW}}{\partial t} = -q_{WW} \tag{20}$$

$$\frac{\partial C_F}{\partial t} = Y_F q_{WW} - r_{ina,F} \tag{21}$$

$$V_{a,b}\left(\frac{\partial S_{Ac,bulk}}{\partial t}\right) = Y_{Ac} q_{WW} V_{a,b} - q_{Ac,AM,bulk} V_{a,b} - A_s J_{s,Ac} \tag{22}$$

$$\frac{\partial C_{AM}}{\partial t} = Y_{AM} q_{Ac,AM,bulk} - r_{ina,bulk,AM} \tag{23}$$

### 2. 4. The boundary conditions of potential equation

The potential equation (Equation 19) requires two boundary conditions. As electrons cannot be transferred to the anolyte, one of the boundary conditions for Equation (23) can be satisfied by the following equation:

$$\frac{d\eta}{dz}|_{z=L_f} = 0 \tag{24}$$

The second form of boundary condition is determined depending on the type of MXC used as a bioenergy generator (including MFC or MEC) and the anode surface potential. The actual cell voltage and electric current can be illustrated by Equation (25) and (26), respectively [14]:

$$V_{cell} = V_{cat} - V_{anod} - I R_{ohm} \tag{25}$$

$$I = A_s j \tag{26}$$

Finally, by combination of Equation (18), (25) and (26), the generalized form of the second boundary condition can be described by:

$$\eta|_{z=0} - \left(A_{anod}.\kappa_{bio}.R_{ohm}\right)\frac{d\eta}{dz}|_{z=0} = V_{cat} - E_{KA} - V_{cell} \begin{cases} V_{cell} = I\,R_{ext} \\ for\ MFC\ Modeling \\ V_{cell} = -V_{app} \\ for\ MFC\ Modeling \end{cases} \quad (27)$$

Hydrogen production rate is a function of generated current as expressed by the following expression [21]:

$$Q_{H_2} = \frac{RT}{V_{a,b}P}\left(\frac{\tau I}{nF}Y_C\right) \quad (28)$$

Notice: Parameters are described in Table 1 and the nomenclature table.

## 3. Results and discussion

### 3. 1. Model Validation

The model validation was conducted with the experimental results from an MFC fed with cheese whey wastewater [22]. Figure 2 illustrates the MFC voltage evolution versus time at the external load of 100 Ω with diluted cheese whey as feed (0.73 $kgCOD.m^{-3}$). The parameters used in this simulation are represented in Table 1. According to Figure 2,

**Table 1. Parameters description and value.**

| Parameter | Description | Value | Unit | Reference |
|---|---|---|---|---|
| $q_{WW,max}$ | maximum uptake rate of wastewater by fermentative bacteria | 72 | $kgCOD_S.kgCOD_X^{-1}.day^{-1}$ | Estimated |
| $q_{AC,E,max}$ | maximum uptake rate of acetate by electrogens | 9.04 | $kgCOD_S.kgCOD_X^{-1}.day^{-1}$ | [9] |
| $q_{AC,AM,max}$ | maximum uptake rate of acetate by acetoclastic methanogens | 8 | $kgCOD_S.kgCOD_X^{-1}.day^{-1}$ | [28] |
| $K_{WW}$ | Monod half-saturation constant of wastewater | 0.5 | $kgCOD_S.m^{-3}$ | [29] |
| $K_{Ac,E}$ | Monod half-saturation constants of acetate consumed by electrogens | 0.001 | $kgCOD_S.m^{-3}$ | [9] |
| $K_{Ac,AM}$ | Monod half-saturation constants of acetate consumed by acetoclastic methanogens | 0.15 | $kgCOD_S.m^{-3}$ | [28] |
| $Y_F$ | yield coefficient of fermentative microorganism production | 0.06 | $kgCOD_X.kgCOD_S^{-1}$ | Estimated |
| $Y_{Ac}$ | yield coefficient of acetate production | 0.4 | $kgCOD_S.kgCOD_S^{-1}$ | Estimated |
| $Y_E$ | yield coefficient of electrogens production | 0.068 | $kgCOD_X.kgCOD_S^{-1}$ | [9] |

**Table 1. Parameters description and value, contiued.**

| Parameter | Description | Value | Unit | Reference |
|---|---|---|---|---|
| $Y_{AM}$ | yield coefficient of methanogens production | 0.05 | $kgCOD_X.kgCOD_S^{-1}$ | [28] |
| $Y_C$ | dimensionless cathode efficiency | 0.8 | Dimensionless | Estimated |
| $b_{ina,F}$ | fermentative bacteria inactivation rate constant | 0.02 | $day^{-1}$ | Estimated |
| $b_{ina,E}$ | electrogens inactivation rate constant | 0.02 | $day^{-1}$ | [30] |
| $b_{ina,AM}$ | bulk acetoclastic methanogens inactivation rate constant | 0.02 | $day^{-1}$ | [28] |
| $b_{res}$ | endogenous respiration reaction constant | 0.07 | $day^{-1}$ | [13] |
| $b_{det}$ | detachment constant | 0.05 | $day^{-1}$ | [13] |
| $E_{KA}$ | half maximum rate potential | -0.85 | V | Estimated |
| $R_{ohm}$ | Ohmic resistance | 2000 | Ω | [22] |
| $D_{Ac,l}$ | diffusion coefficient of acetate in the anolyte | 0.941 | $cm^2.day^{-1}$ | [31] |
| $D_{Ac,f}$ | diffusion coefficient of acetate in the biofilm | 0.753 | $cm^2.day^{-1}$ | [32] |
| $\gamma_1$ | electron generated by substrate consumption | 125 | $mole\text{-}.kgCOD_S^{-1}$ | [30] |
| $\gamma_2$ | electron generated through the endogenous respiration | 125.006 | $mole\text{-}.kgCOD_X^{-1}$ | [30] |
| $V_{a,b}$ | anode compartment liquid volume | 250 | $cm^3$ | [22] |
| $A_s$ | anode surface area | 13.8 | $cm^2$ | [22] |
| $f_e^0$ | fraction of energy-generating electrons | 0.9 | Dimensionless | [30] |
| $\kappa_{bio}$ | biofilm conductivity | 0.05 | $S.m^{-1}$ | [33] |
| $X_{j,a}$, $X_{j,i}$ | active and inactive biomass density of microorganism j | 300 | $kgCOD_x.m^{-3}$ | [9] |
| F | Faraday's constant | 96485 | $Coulomb.mole\text{-}^{-1}$ | [31] |
| R | universal gas constant | 8.314 | $J.mol^{-1}.K^{-1}$ | [31] |
| τ | time conversion factor | 86400 | $s.day^{-1}$ | [13] |
| n | number of electrons transferred | 2 | $mole\text{-}.mol^{-1}\text{-}H_2$ | [15] |

**Table 1. Parameters description and value, contiued.**

| Parameter | Description | Value | Unit | Reference |
|---|---|---|---|---|
| $pH_{UL,E}$ | Upper limit of pH for electrogens growth | 8.2 | Dimensionless | [24] |
| $pH_{LL,E}$ | Lower limit of pH for electrogens growth | 7.2 | Dimensionless | [24] |
| $pH_{UL,AM}$ | Upper limit of pH for acetoclastic methanogens growth | 6.5 | Dimensionless | [18] |
| $pH_{LL,AM}$ | Lower limit of pH for acetoclastic methanogens growth | 7.5 | Dimensionless | [18] |
| $pH_{UL,F}$ | Upper limit of pH for fermentative bacteria growth | 5.2 | Dimensionless | [27] |
| $pH_{LL,F}$ | Lower limit of pH for fermentative bacteria growth | 6.5 | Dimensionless | [27] |

as the microbial consortium was employed from the cheese whey wastewater activated sludge [22] the voltage reached a maximum of approximately 50 mV in the first cycle and remained constant in the second cycle. The variations of cheese whey wastewater and acetate bulk concentrations as well as the wastewater experimental measurements are depicted in Figure 3. Since initial conditions were estimated based on the trial and error method, measured and simulated values did not incipiently coincided [14]. Moreover, the model predicted the total wastewater consumed in each cycle and it is probably because of the single step fermentation assumption. (Unclear) In other words, according to the measurements, at around 50 and 120 hours in the first and second cycles, fermentation assumption. (Unclear) In other words, according to the measurements, at around 50 and 120 hours in the first and second cycles, respectively, it can be argued that the main part of cheese whey wastewater was

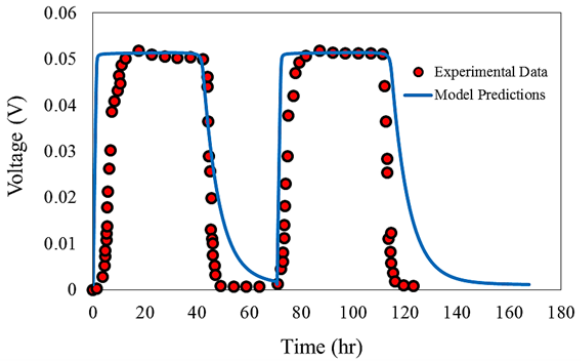


**Fig. 2. Model predictions and experimental data [22] of Voltage evolution in the cheese whey-fed MFC.**

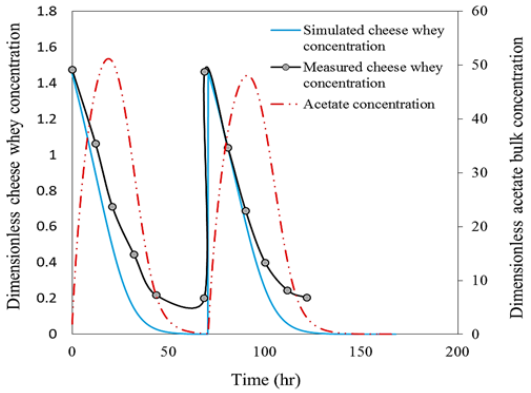


Fig. 3. Model predictions and experimental data [22] of substrates bulk concentrations in the cheese whey-fed MFC.

degraded and after that, the other anaerobic digestion steps like acidogenesis were controlled.

### 3. 2. Effect of applied voltage and cathode potential on hydrogen production and microbial behavior

The preceding MFC can be altered to an MEC by shifting the potential boundary condition. To appraise such an MEC, the effect of applied voltage at the cathode potential of -0.8 V and cathode surface potential at the applied voltage of 0.9 V on the hydrogen production rate were simulated with the same initial conditions and feed concentration and the results are shown in Figure 4. As information given in this figure shows, a higher hydrogen production rate was attainable at the higher applied voltage and cathode surface potential which is corroborated by experiment [6]; but that by exerting the external applied voltage of 0.9 V and poising more positively the cathode surface potential the hydrogen production rate noticeable increased. The main reason for this can be inferred from the variation of anode surface potential which directly affects the biofilm status and the microbial population. For this purpose, the anode surface potential, after 4 days when the system reached a steady state, were simulated at the different cathode surface potentials. As Figure 4 reveals, the higher cathode potential provided more positive anode potentials and this is symptomatic of more energy gainfrom the enhancement of electrogenic activity [23].

In conclusion, the further current to produce hydrogen is afforded (unclear). Furthermore, as depicted in Figure 5, the conductive biofilm at the poised cathode potential of 0.9 V has a higher electrogens and the lower methanogens content in comparison with the poised cathode potential of 0.2 V. Additionally in this simulation, with the same initial conditions the influence of cathode surface potential on the liquid bulk was extremely slight, so that after 2 days the ratio of the bulk acetoclastic methanogens at 0.2 per 0.9 V cathode potential was 1.005 and 1 for fermentative microorganisms. It can be argued that when initial wastewater and microbial concentrations at different cathode potentials are equal, bulk microbes behave independently with respect to the cathode potential. Therefore, depending in large part on the MEC construction and economics, modeling can predict the optimum conditions through different ways to increase the hydrogen production.

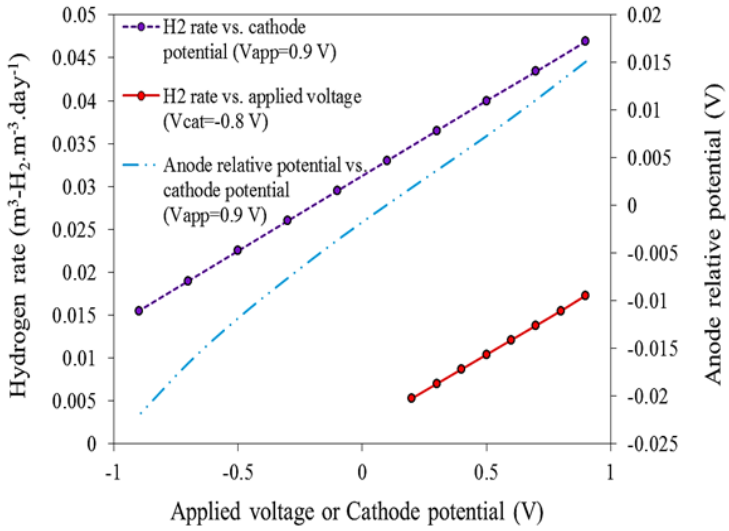


**Figure 4. The effect of applied voltage and cathode potential on the final hydrogen rate and anode relative potential variation versus cathode potential in the supposed cheese whey-fed MEC.**

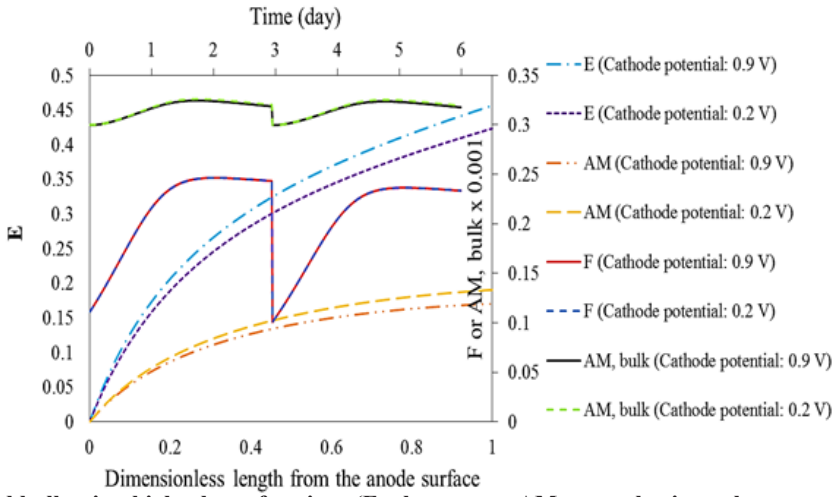


**Fig. 5. Biofilm and bulk microbial volume fractions (E: electrogens, AM: acetoclastic methanogens, F: fermentative bacteria, AM, bulk: bulk acetoclastic methanogens) at the poised cathode potentials of 0.2 and 0.9 V with the applied voltage of 0.9 V and the same initial conditions.**

### 3. 3. Effect of pH on power generation and microbial behavior

It would be interesting to investigate the influence of pH on biolectrochemical systems. Operating pH is one of the important aspects to optimize power generation. For this purpose, we changed the operating pH from 5.5 to 10 to survey the cheese whey-fed MFC performance under load 100 Ω and the same conditions described in Section 3.1. The average power density (calculated by $V_{cell}^2/R_{ext}$ ) during 168 hours as a function of pH is shown in Figure 6. As indicated, the maximum of average power density of 17.71 $mW.m^{-2}$ was attained at approximately the pH of 7.5 and the optimum range for generating power was from 7 to 8.

The biocatalyst formed on the anode surface has the main role in the power generation; hence, the microbial behavior in the biofilm as well as the biofilm thickness were simulated under pH variations. Figure 7 represents the average volume fractions of electrogens and acetoclastic methanogens. The optimum pH for growth of electrogens and acetoclastic methanogens is 7.7 [24] and 7 [18], respectively. But in a mixed culture with rival microbial groups the optimum pH changed. As acetoclastic methanogens have a slow growth rate [25, 26] in comparison with electrogens, the optimum pH for electrogens was not changed

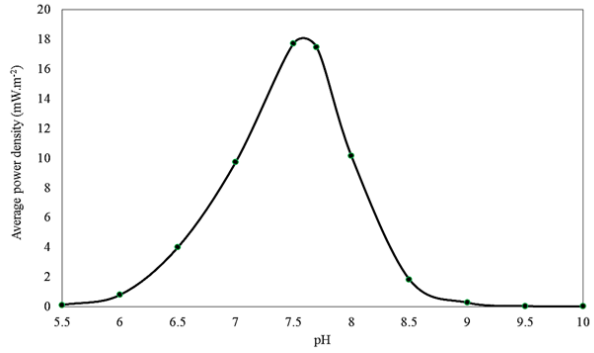


**Fig. 6. The average power density during 168 hours as a function of pH.**

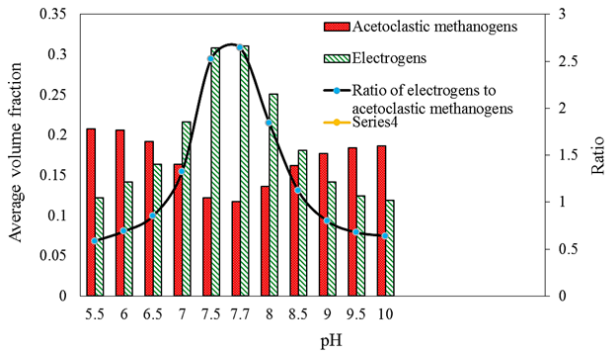


**Fig. 7. The average volume fractions of electrogens and acetoclastic methanogens as a function of pH.**

(7.7), while the acetoclastic methanogens volume fraction in the biofilm was more in the pH of 5.5, 6, 6.5, 9, 9.5 and 10 with the highest growth found in pH

5.5 (not 7) where the growth of electrogens was the lowest.

The final biofilm thickness in each pH is shown Figure 8. The maximum thickness of the biocatalyst was 13.74 μm in the pH of 7.5. In addition, as shown in this figure, in that pH the highest volume fraction of the active biomass in the biofilm was gained.

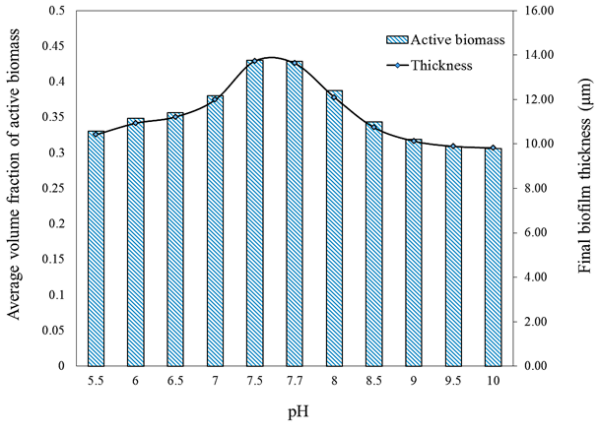


**Fig. 8. The variation of average volume fraction of active biomass and final biofilm thickness versus pH.**

In addition to biofilm the anolyte, as a place where wastewater is decomposed and acetate is produced, influences the power output. In Figure 9 the variation of the average volume fractions of acetoclastic methanogens and fermentative bacteria as well as the average dimensionless acetate concentration in the anolyte are depicted. In the optimum pH range of 5.2 to 6.5 for fermentative bacteria [27], the electrogenic activity of the biofilm was low (Figure 7), so acetate was consumed at a lower rate by electrogens, and consequently, it accumulated in the anolyte. Therefore, in the optimum pH range of 6.5 to 7.5 for acetoclastic methanogens [18] the volume fraction of these microbes in the anolyte was high. By increasing the electrogenic activity of the biofilm for pH values above 7 (Figure 7), acetatewas diffused and consumed more rapidly in the biocatalyst, and as a consequence, power increased (Figure 6). For more alkaline anodic pH (above 8), the activity of fermentative bacteria and acetate production was reduced, while acetoclastic methanogens remained active in both anolyte and biofilm; thus acetate bulk concentration diminished.

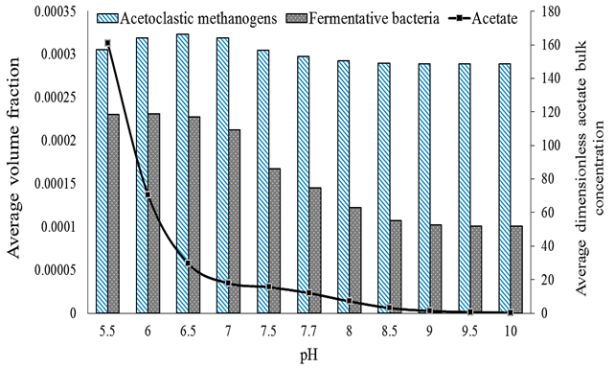


**Fig. 9. The variation of the average volume fractions of acetoclastic methanogens and fermentative bacteria as well as the average dimensionless acetate concentration in the anolyte versus pH.**

## 4. Conclusion

In this study a general model to evaluate both MFCs and MECs was extended. Model prediction was in agreement with experimental results for a complex wastewater (i.e. cheese whey wastewater). Measured and simulated cheese whey concentrations revealed the same trend, especially at the initial time of each cycle. In the cheese whey-fed MEC, both applied voltage and poising cathode surface potential had a similar effect on the MEC performance, but the effect of cathode surface potential at the applied voltage of 0.9 V represented a better optimum hydrogen production rate. On the other hand, higher electrogens activity and more positive anode surface potential were obtained at the more positive cathode surface potential, and in contrast, methanogens activity was reduced. At the same initial conditions the bulk microorganisms activity was relatively independent to the cathode surface potential. Operating pH sharply affected the performance of the bioelectrochemical system. Optimum pH for electrogens did not change (pH 7.7), but due to the lower growth rate of acetoclastic methanogens the amount of this group increased in acidic (5.5) and alkaline (10) pH. Power output, biofilm thickness and biofilm active biomass were maximized in the pH of 7.5. For pH values below

7 acetate accumulated in the anolyte on account of the higher fermentative activity and lower electrogenic activity, it diminished between pH of 7 to 8 due to the higher electrogenic activity, and also above a pH of 8 owing to the lower fermentative activity. Eventually, further work, such as considering the effect of hydrogenotrophic methanogens and multi-step anaerobic digestion modeling, is required to acquire a more comprehensive model.

## 5. Acknowledgement

This research was supported by Sharif University of Technology, Vice President for Research Grant G930111.

## Nomenclature

| | |
|---|---|
| q | substrate consumption rate in the liquid bulk ($kgCOD_S.day^{-1}$) or in the biofilm ($kgCOD_S.kgCODX^{-1}.day^{-1}$) |
| C | suspended microorganism concentration ($kgCOD_x.m^{-3}$) |
| $\phi$ | microorganism volume fraction in the biofilm (dimensionless) |
| S | substrate concentration ($kgCOD_S.m^{-3}$) |
| K | Monod half-saturation constant ($kgCOD_S.m^{-3}$) |
| r | inactivation and endogenous respiration rate ($day^{-1}$) |
| b | inactivation, endogenous respiration and detachment constant ($day^{-1}$) |
| F | Faraday's constant (Coulomb.mole-$^{-1}$) |
| R | universal gas constant ($J.mol^{-1}.K^{-1}$) |
| T | temperature (K) |
| P | pressure (Pa) |
| $\eta$ | local electrical potential of the biofilm (V) |
| $E_{KA}$ | half maximum rate potential (V) |
| D | diffusion coefficient ($m^2.day^{-1}$) |
| X | biomass density ($kgCOD_X.m^{-3}$) |
| L | thickness (m) |
| Y | biomass ($kgCOD_X.kgCOD_S^{-1}$) and acetate yield coefficients |
| $Y_C$ | dimensionless cathode efficiency |
| $\mu$ | net specific growth rate ($day^{-1}$) |
| v | advective velocity ($m.s^{-1}$) |
| Q | volumetric rate ($m^3.m^{-3}$-anolyte.$day^{-1}$) |
| $V_{a,b}$ | anode compartment liquid volume ($m^3$) |
| $A_s$ | surface area ($m^2$) |
| $J_s$ | mass flux ($kgCOD_S.m^{-2}.day^{-1}$) |
| j | current density ($A.m^{-2}$) |
| $K_{bio}$ | biofilm conductivity ($S.m^{-1}$) |
| $\gamma$ | electron equivalence of substrate or biomass (mole-.$kgCOD^{-1}$) |
| $f_e^0$ | fraction of energy-generating electrons (dimensionless) |
| $\tau$ | time conversion factor ($s.day^{-1}$) |
| V | actual voltage (V) |
| I | current (A) |
| R | electrical resistance ($\Omega$) |
| n | number of electrons transferred (mole-.mol-1-$H_2$) |
| z | spatial longitudinal coordinate from the anode surface (m) |
| t | time (day) |

## Subscript

| | |
|---|---|
| *S* | substrate |
| *X* | biomass |
| *WW* | wastewater |
| *Ac* | acetate |
| *E* | electrogenic microorganism |
| *AM* | acetoclastic methanogens |
| *a* | active biomass |
| *i* | inactive biomass |
| *f* | biofilm |
| *l* | liquid |
| *det* | detachment |
| *ext* | external |
| *ohm* | ohmic |
| *cell* | fuel cell |
| *anod* | anode |
| *cat* | cathode |

| | |
|---|---|
| $H_2$ | hydrogen |
| *max* | maximum |
| *app* | applied voltage |
| *bulk* | liquid bulk |
| *surface* | liquid/biofilm interface |
| *res* | endogenous respiration |
| *ina* | inactivation |
| *LL* | lower limit |
| *UL* | upper limit |

## 6. References

[1] Rozendal R. A., Hamelers H. V. M., Euverink G. J. W., Metz S. J., Buisman C. J. N., "Principle and perspectives of hydrogen production through biocatalyzed electrolysis", Int. J. Hydrogen Energy 2006, 31: 1632.

[2] Mardanpour M. M., Esfahany M. N., Behzad T. and Sedaqatvand R., "Single chamber microbial fuel cell with spiral anode for dairy wastewater treatment", Biosens. Bioelectron., 2012, 38: 264.

[3] Logan B. E., "Microbial Fuel Cells", Wiley, 2008.

[4] Liu H., Grot S. and Logan B. E., "Electrochemically assisted microbial production of hydrogen from acetate", Environ. Sci. Technol., 2005, 39: 4317.

[5] Wang A., Sun D., Cao G., Wang H., Ren N. and Wu W.M. et al., "Integrated hydrogen production process from cellulose by combining dark fermentation microbial fuel cells and a microbial electrolysis cell", Bioresour. Technol., 2011, 102: 4137.

[6] Cheng S. and Logan B. E., "Sustainable and efficient biohydrogen production via electrohydrogenesis", Proc. Natl. Acad. Sci., 2007, 104: 18871.

[7] Farhangi S., Ebrahimi S. and Niasar M., "Commercial materials as cathode for hydrogen production in microbial electrolysis cell", Biotechnol. Lett., 2014, 36: 1987.

[8] Nam J.-Y., Tokash J. C. and Logan B. E., "Comparison of microbial electrolysis cells operated with added voltage or by setting the anode potential", Int. J. Hydrogen Energy, 2011, 36: 10550.

[9] Picioreanu C., Head I. M., Katuri K. P., van Loosdrecht M. C. M. and Scott K., "A computational model for biofilm-based microbial fuel cells", Water Res., 2007, 41: 2921.

[10] Picioreanu C., Katuri K. P., Head I. M., Loosdrecht M. C. M. v. and Scott K., "Mathematical model for microbial fuel cells with anodic biofilms and anaerobic digestion", Water Sci. Technol. 2008, 57.

[11] Picioreanu C., van Loosdrecht M. C. M., Curtis T. P. and Scott K., "Model based evaluation of the effect of pH and electrode geometry on microbial fuel cell performance", Bioelectrochemistry 2010, 78: 8.

[12] Pinto R. P., Srinivasan B., Manuel M. F. and Tartakovsky B., "A two-population bio-electrochemical model of a microbial fuel cell", Bioresour. Technol., 2010, 101: 5256.

[13] Kato Marcus A., Torres C. I. and Rittmann B. E., "Conduction-based modeling of the biofilm anode of a microbial fuel cell", Biotechnol. Bioeng., 2007, 98: 1171.

[14] Sedaqatvand R., Nasr Esfahany M., Behzad T., Mohseni M. and Mardanpour M. M., "Parameter estimation and characterization of a single-chamber microbial fuel cell for dairy wastewater treatment", Bioresour. Technol., 2013, 146: 247.

[15] Pinto R. P., Srinivasan B., Escapa A. and Tartakovsky B., "Multi-population model of a microbial electrolysis cell", Environ. Sci. Technol., 2011, 45: 5039.

[16] Usack J. G. and Angenent L. T., "Comparing the inhibitory thresholds of dairy manure co-digesters after prolonged acclimation periods: Part 1 – Performance and operating limits", Water Reach, in press.

[17] Qiao W., Takayanagi K., Shofie M., Niu Q., Yu H. Q. and Li Y.-Y., "Thermophilic anaerobic digestion of coffee

grounds with and without waste activated sludge as co-substrate using a submerged AnMBR: System amendments and membrane performance", Bioresour. Technol., 2013, 150: 249.

[18] D.J. Batstone J. K., Angelidaki I., Kalyuzhnyi S.V., Pavlostathis S.G., Rozzi A., W.T.M. Sanders H. S. and Vavilin V.A., "The IWA Anaerobic Digestion Model No 1 (ADM1)", Water Sci. Technol., 2002, 45: 65.

[19] Wanner O. and Gujer W., "A multispecies biofilm model", Biotechnol. Bioeng., 1986, 28: 314.

[20] Bernardi D. M. and Verbrugge M. W., "Mathematical model of a gas diffusion electrode bonded to a polymer electrolyte", AICHE J., 1991, 37: 1151.

[21] Pinto R. P., Tartakovsky B. and Srinivasan B., "Optimizing energy productivity of microbial electrochemical cells", J. Process Contr., 2012, 22: 1079.

[22] Antonopoulou G., Stamatelatou K., Bebelis S. and Lyberatos G., "Electricity generation from synthetic substrates and cheese whey using a two chamber microbial fuel cell", Biochem. Eng. J., 2010, 50: 10.

[23] Zhang L., Zhu X., Li J., Liao Q. and Ye D., "Biofilm formation and electricity generation of a microbial fuel cell started up under different external resistances", J. Power Sources 2011, 196: 6029.

[24] Marcus A. K., Torres C. I. and Rittmann B. E., "Evaluating the impacts of migration in the biofilm anode using the model PCBIOFILM", Electrochim. Acta, 2010, 55: 6964.

[25] Peng J., Lü Z., Rui J. and Lu Y., "Dynamics of the methanogenic archaeal community during plant residue decomposition in an anoxic rice field soil", Appl. Environ. Microbiol. 2008, 74: 2894.

[26] Jung S. and Regan J. M., "Influence of external resistance on electrogenesis, methanogenesis, and anode prokaryotic communities in microbial fuel cells", Appl. Environ. Microbiol. 2011, 77: 564.

[27] R. Solera L. I. R., D. Sales., "The evolution of biomass in a two-phase anaerobic treatment process during start-up", Chem. Biochem. Engin. Q., 2002, 16: 25.